



Optimization of photocatalytic degradation of β -naphthol using nano TiO₂-activated carbon composite

Hossein Ijadpanah-Saravi^a, Saeed Dehestaniathar^{b,*}, Ahmad Khodadadi^a, Mehdi Safari^c

^aFaculty of Engineering, Department of Environmental Engineering, Tarbiat Modares University, Tehran, Iran, Tel. +98 9303162646; email: hossein.ijad@gmail.com (H. Ijadpanah-Saravi), Tel. +98 9123908067; email: akdarban@modares.ac.ir (A. Khodadadi)

^bKurdistan Environmental Health Research Center, Kurdistan University of Medical Sciences, Sanandaj, Iran, Tel. +98 9127100737; email: saeed_dehestani@yahoo.com

^cFaculty of Petroleum Engineering, Department of Petroleum Engineering, Amirkabir University of Technology, Tehran, Iran, Tel. +98 9365552919; email: Safari.mehdi@gmail.com

Received 20 July 2014; Accepted 27 November 2014

ABSTRACT

β -naphthol is a highly toxic compound and up to now, various approaches were proposed to remove it. However, these methods indicate low removal efficiencies since these materials are difficult to degrad. Hence, this research aims to synthesize TiO₂ nanoparticles with maximum photocatalytic properties suitable for application in the β -naphthol wastewater treatment. For this purpose, firstly, two types of titanium nanoparticles in the crystalline forms of anatase and rutile were synthesized. Here, anatase crystals indicated superior photocatalytic properties, as compared to the rutile crystals. The hypothesis behind this work is that using a biphasic mixture of the rutile and the anatase may enhance the photocatalytic properties of the anatase. Then these synthesized nanoparticles were stabilized on activated carbon (AC) using the microwave thermal stabilization. Next, characterization of these nanoparticles was performed using the X-ray diffraction and scanning electron microscopy techniques. The results indicated when having the ratio of 4:1 anatase to rutile, this nano-TiO₂ stabilized on AC indicate the maximum catalytic activity in β -naphthol degradation. In addition, at pH 11, catalyst content of 8 g/L, and aeration of 0.36 m³/h, the maximum β -naphthol removal was observed. The complete removal of β -naphthol from the initial solution occurred in a duration shorter than 90 min using the initial concentration of C₀ = 3 × 10⁻⁴ mol/L.

Keywords: Photocatalyst; Nano-TiO₂; Photocatalytic degradation; Beta-naphthol; Activated carbon

1. Introduction

Polycyclic aromatic hydrocarbons (PAHs) are a group of organic compounds with two or several

benzene cycles [1]. The carcinogenic and mutative effects and the high toxicity of these substances have highlighted the necessity for their recycling from the industrial wastes [2]. The conventional water and wastewater treatment methods indicate low efficiency in their removal, since these materials are difficult to

*Corresponding author.

degrad [3]. Hence, in the recent years, many researchers have concentrated their efforts on the application of advanced oxidation process techniques for the removal of aromatic compounds [3–5]. Among the various approaches of this technique, photocatalytic oxidation using the nano photocatalytics is a very effective technology [6] which is performed using the UV radiation on the surface of a semi-conductive material such as TiO_2 [7–10] and ZnO [11–14]. This method is based on irradiation of UV light to the TiO_2 surface, which leads to electron excitation from their valance layer to the conductance layer. Therefore, an electron–hole pair is created. Some of these pairs are removed by their recombination on the surface of the bulk crystal and the remaining pairs diffuse into the crystalline surface. Then, an electro-philic species such as oxygen adsorbs the electrons on the catalyst surface and results in the creation of super-oxide radicals. Besides, the remaining hole also takes an electron from OH^- existing in the environment and produces a hydroxyl radical, as a result. This hydroxyl radical is highly active and causes destruction of the hardly degradable structures such as benzene cycles through hydrogen absorbing from organic compounds [7,15–19].

As a member of PAHs family, β -naphthol, $\text{C}_{10}\text{H}_7\text{OH}$, has a plenty of applications in the chemical dyes industry, pharmaceutical industry, pesticides, and plastic production. A large amount of β -naphthol annually enters to the aquatic ecosystems through the industrial wastes. The maximum allowable amount of this compound in the effluent of the factories is 3 ppm.

Recently, several researchers [2,20–24] have studied the photocatalytic degradation of β -naphthol by nano- TiO_2 [24,25] and reported that the contaminant molecule's absorbance on a catalyst surface enhances its catalytic performance by absorbing the precursor of photo-degradation reaction. Since the majority of the commercial nano- TiO_2 has the specific surface area below $50 \text{ m}^2/\text{g}$, they have less adsorption potential as compared to the compounds with weak polarity such as aromatics and phenols. This implies that the removal efficiency is controlled by these nanoparticles [26–28]. One method for dealing with shortcomings is to absorb more contaminants around the catalyst through stabilization of nano- TiO_2 on activated carbon (AC), as it involves a very high absorption potential. This results in an increase in the removal efficiency, particularly for drinking water treatment, because of the low concentration of the contaminants [29]. Moreover, the intermediate substances produced from photocatalytic degradation are quickly absorbed by the AC. Consequently, the next steps of

photo-degradation are performed on them, whereby, they are degraded to CO_2 and H_2O [30]. Hence, the secondary pollutant induced by the side products is minimized. Through this method, recycling the AC-containing nano- TiO_2 from the solution as deposition problem induced by the fine size of these nanoparticles no longer exists. In the past few years, a large number of studies have been performed using various stabilization techniques of nano- TiO_2 on AC for contamination removal [30]. Fig. 1 depicts a schematic illustration of TiO_2 stabilized on AC and the way the contaminant is adsorbed on it.

Titanium dioxide is found in the amorphous form and there exist three crystalline phases which are anatase, rutile, and brookite. Each of them has its own unique properties. Rutile is stable at the ambient temperature. However, Anatase and brookite are semi-stable and could convert to rutile at appropriate temperature conditions. Existing sulfate ion causes the ratio of rutile to anatase to vary. Although anatase nanoparticles show stronger photocatalytic activity as compared to rutile nanoparticles, anatase and rutile phases being together may improve the photocatalytic properties of anatase, as it confines a larger number of electrons in its structure compared to rutile. It is expected that by adding the rutile phase to anatase, electron transfer from anatase to rutile occurs in an easier fashion and a larger number of hydroxyl groups discharge from plains (101) and (001) of anatase [16,29,31,32].

In this study, firstly, the relatively cheap and accurately controlled hydrolysis of TiCl_4 is applied to synthesize rutile and anatase crystals with various ratios. Next, these nanoparticles were stabilized on AC

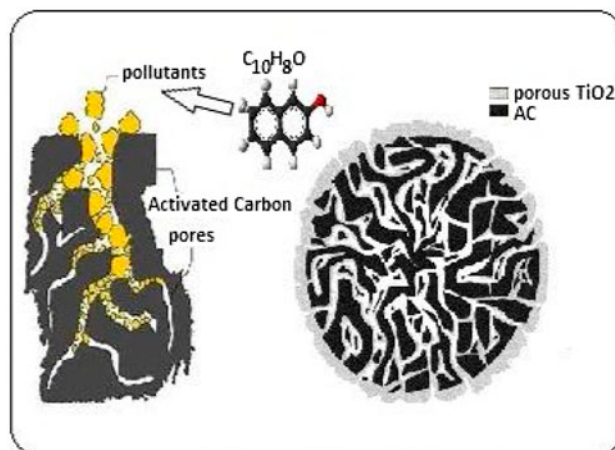


Fig. 1. Schematic illustration of nanoparticles coating on surface of AC and the process of adsorption of the contaminant by activated carbon.

using microwave energy. Finally, the performance of the produced catalyst was examined on β -naphthol removal. To achieve the best photo-degradation efficiency, determination of the optimum ratio of anatase phase to rutile phase is essential. Moreover, the effects of various parameters such as catalyst content, aeration, solution acidity, and concentration of β -naphthol were studied. In addition, a comparison was made between the adsorption, photocatalytic degradation, and photo-degradation processes and their synergic effect on β -naphthol degradation.

2. Materials and methods

2.1. Materials

All chemicals used in this research were selected from among those with high purity level. Titanium tetrachloride, ammonium hydroxide, ammonium sulfate, sodium hydroxide, and β -naphthol were supplied all by Merck Inc., Germany (purity $\geq 99\%$). The granola AC was purchased with grain size of 0.1–0.3 mm from Iran Sanat Carbon Inc., and then washed with distilled water for initial preparation. Then, it was dried for 8 h at 110°C.

2.2. Preparation

Titanium nanoparticles introduced in this work were synthesized in crystalline forms of anatase, rutile, and biphasic mix of anatase with rutile through the controlled hydrolysis of titanium tetrachloride [33–35]. To simultaneously synthesize rutile and anatase phases, a small amount of ammonium sulfate was added to the titanium tetrachloride solution. To stabilize these nanoparticles on AC, 4 g of TiO_2 was dispersed in 100 mL ethanol and then the solution pH was adjusted to 3 using the diluted nitric acid. Next, for complete dispersion of the crystals, the obtained mix was placed in the ultrasonic apparatus for 15 min. After that, during 2 h, 10 g AC was added to the mix and it was gradually agitated using the magnet agitator. For thermal stabilization, the obtained solution was put in the microwave with power 180 W and temperature 250°C at vacuum conditions. For complete deposition of the nanoparticles on the surface of the AC, the process was repeated twice more.

2.3. Photo-reactor

The photo-reactor used in this work contains a cylindrical reactor equipped with a radiation and aeration system. Fig. 2 presents a schematic view of this photo-reactor. The height and diameter of the reactor

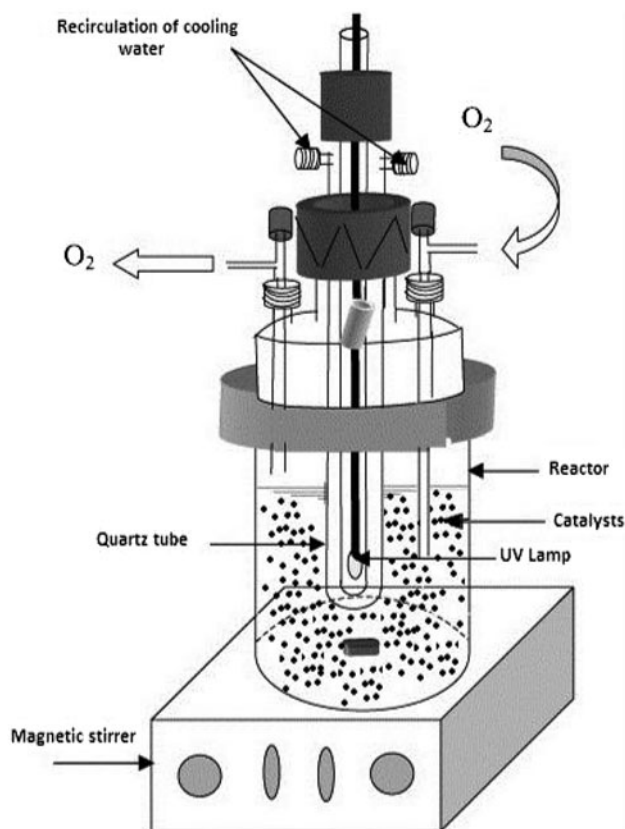


Fig. 2. Schematic drawing of the photo-reactor.

are 35 and 20 cm, respectively. A UV-C light with power 20 W, manufactured by Philips Inc., is used in this reactor.

3. Methodology and analysis

To evaluate the anatase phase to the rutile phase ratio in TiO_2 nanoparticles, X-ray diffraction (XRD) analysis was carried out using a device fabricated by X'pert 1480, Philips Inc., The Netherlands. It was also possible to estimate the anatase to rutile ratio in the samples using the Spurr Meyers equation:

$$X_A(\%) = 100 / (1 + 1.265 \cdot I_R / I_A) \quad (1)$$

$$X_R(\%) = 100 / (1 + 0.8 \cdot I_A / I_R) \quad (2)$$

where I_A is the anatase phase intensity at $2\theta = 25.24$, I_R is the intensity of rutile peak at $2\theta = 27.83$, X_R and X_A are the weight percentage of anatase and rutile in the samples, respectively. To study the shape and morphology of the nanoparticles, scanning electron microscopy (SEM), model: XL30, Philips Inc., was

used. To determine the concentration of the organic volatile complex compounds, gas chromatography (GC) was used. To inject the samples to the GC device, the analyzed material was transferred from the aqueous phase to the organic phase. To do so, first, 10 mL of the sample was mixed with 2 mL of dichloromethane and agitated for 1.5 h. Once the agitation process is stopped, dichloromethane is deposited and segregated since it is heavier. The process was repeated twice more. Then, 6 mL of dichloromethane containing β -naphthol was heated at a mild temperature and the mix volume was reduced to 1 mL. Finally, 1 μ L of the mix was injected to the GC device. Thermal adjustment was performed in the following manner, where the oven temperature was kept at 65°C for 1 min and then it was increased to 210°C with gradient of 15°C/min and kept at this temperature for 3 min. The injector and detector temperatures were adjusted in split less state at 200 and 210°C, respectively.

4. Results and discussion

4.1. Effect of crystal type

To determine the photocatalytic properties among different forms of TiO_2 , firstly, different crystalline forms of anatase, rutile, and biphasic mix of anatase with rutile (with various anatase to rutile ratios of 1, 2, and 4) were synthesized. Then, these nanoparticles were separately stabilized on AC. Next, their effect was examined on β -naphthol removal. Fig. 3 illustrates degradability of β -naphthol by the studied catalysts.

The figure shows that the phase ratio of anatase to rutile of four ($A/R=4$) could result in complete

removal of β -naphthol in 150 min. On the other hand, anatase, $A/R=2$ and 1, and rutile indicated maximum removal of 96.5, 63.5, 50, and 31%, respectively. As a result, the phase ratio of anatase to rutile of four ($A/R=4$) is suggested as the optimum ratio. Therefore, AC coated by the nano- TiO_2 is introduced as the best catalyst. This phenomenon can be attributed to the fact that although photocatalytic property of anatase is higher than that of rutile, a slight amount of rutile added to anatase minimizes the probability of electron-hole recombination and, consequently, leads to an increase in photocatalytic properties of this compound. The optimum ratio of anatase/rutile was used in the following experiments.

4.2. Characteristics of the nano- TiO_2 stabilized on AC

Fig. 4 presents XRD pattern of optimum biphasic mix of anatase with rutile. Based on the calculations performed on the XRD spectrum of the phase mix, it was found that crystalline particles contain 80 and 20% of the anatase and rutile phases, respectively.

As mentioned previously, to study the morphology of the synthesized catalysts, SEM device was used. Fig. 5 depicts the surface of the AC before and after stabilization of $A/R=4$ in various magnifications. The figure demonstrates that stabilization of the nano- TiO_2 on all surfaces was done completely and uniformly.

For the elemental analysis of the nanophotocatalyst, the synthesized samples were analyzed by Energy dispersive X-ray spectrometry (EDX). These EDX spectra of nano TiO_2 -AC composites and nano TiO_2 particles are shown in Fig. 6. These spectra illustrate the existence of C, O, and also strong Ti peaks. In the case of both of the samples, titanium

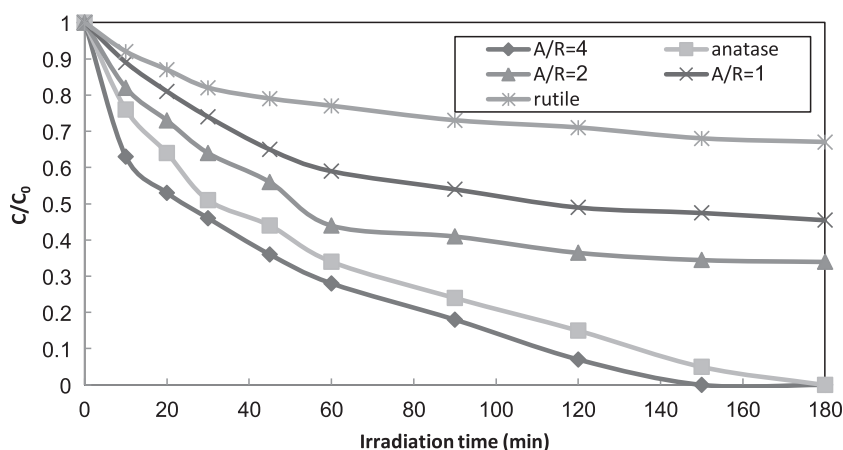


Fig. 3. The role of various anatase to rutile (A/R) ratios stabilized on AC on the photocatalytic degradation of β -naphthol.

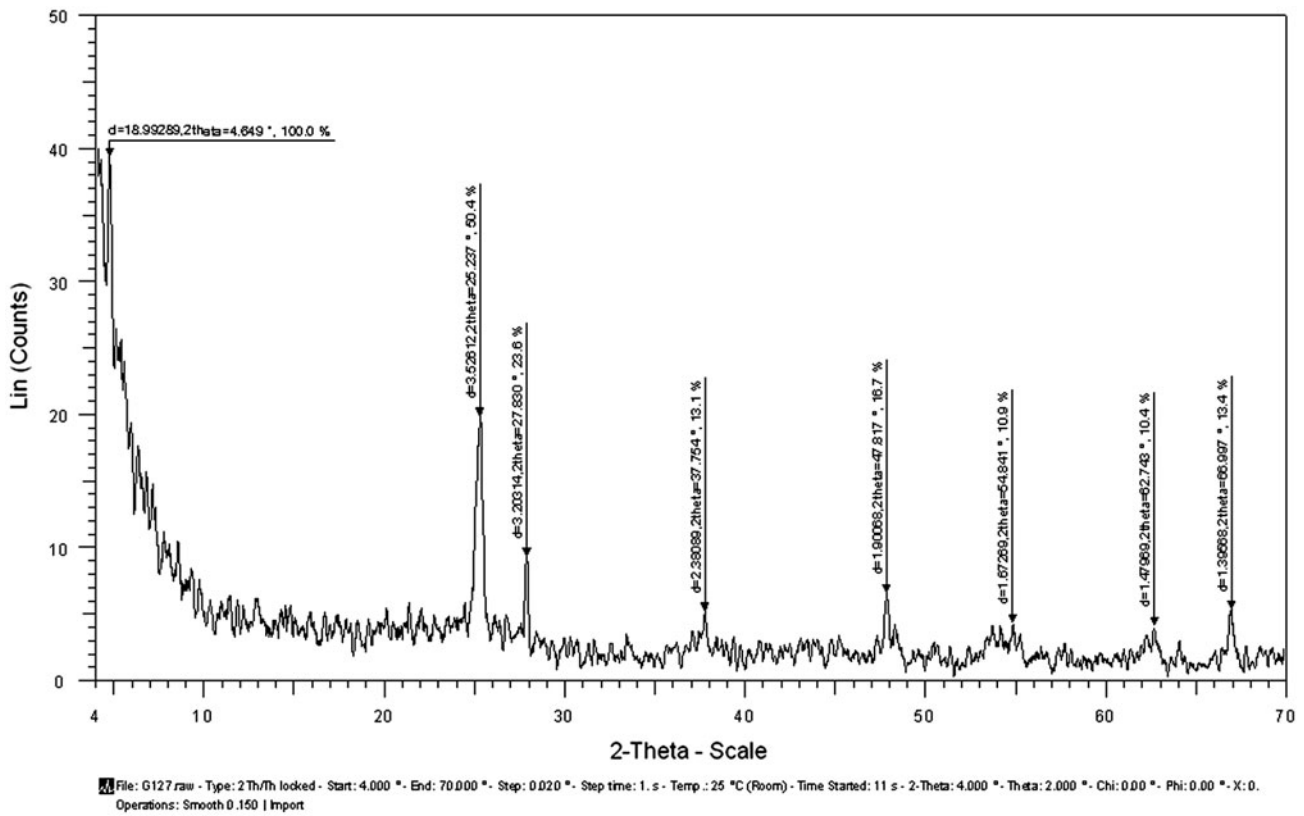


Fig. 4. XRD patterns of the optimum biphasic mix of anatase with rutile.

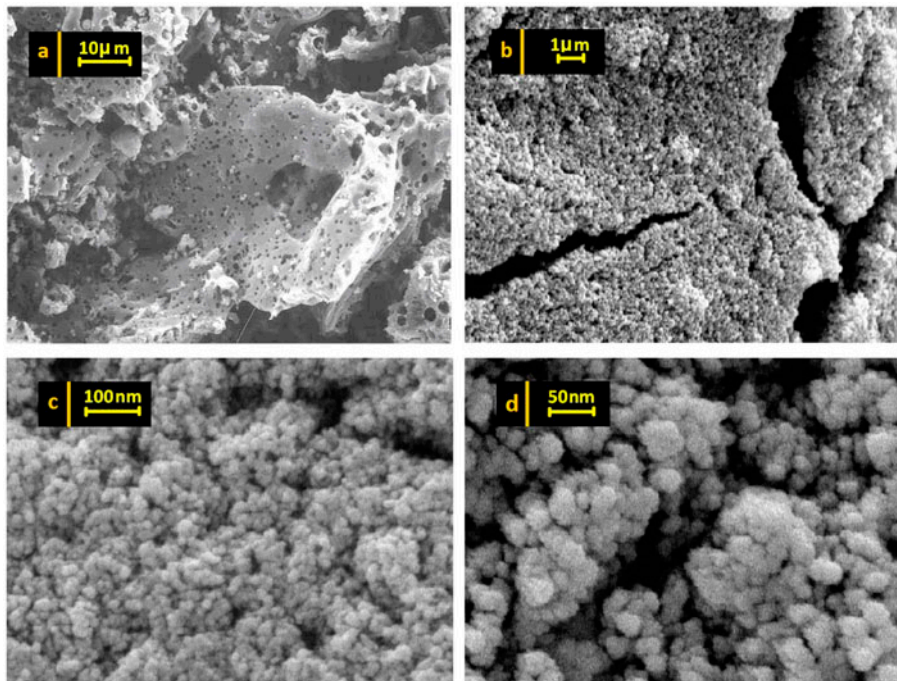


Fig. 5. SEM micrographs of (a) AC and (b)–(d) nano-TiO₂ coated on AC in various magnifications.

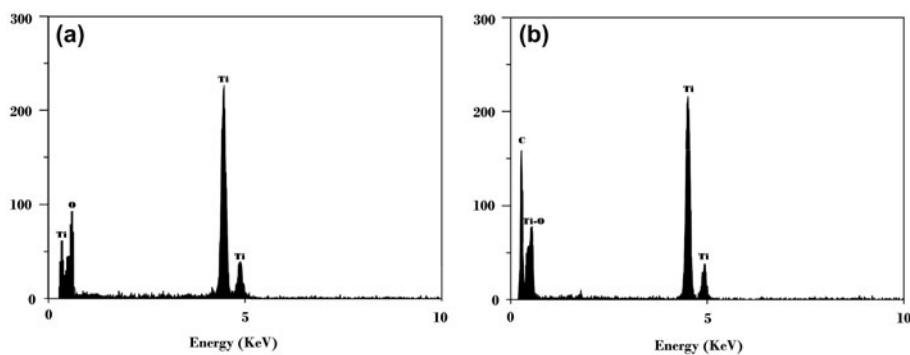


Fig. 6. EDX analysis of TiO₂ nanoparticles (a) and AC-TiO₂ composite (b).

element was introduced as nearly the main element in the samples.

4.3. Optimum content of the catalyst

In this work, the effect of various contents of the best catalyst (AC coated by optimum anatase to rutile ratio) was examined in photocatalytic degradation of a solution containing 5×10^{-4} mol/L of β -naphthol (Fig. 7). As shown in Fig. 7, an increase in the best catalyst from 3 to 7 g/L leads to an increased removal efficiency and then a slight decrease in removal efficiency is observed. This trend can be explained as: Once the best catalyst content rises, the number of free OH radicals and the amount of absorbed contaminants on the best catalysts increase and lead to the increased removal efficiency. However, after particular catalyst content, the created opacity in the solution reduces the UV penetration depth; therefore, the number of radicals is decreased and a slight decrease in the removal

efficiency is observed. In general, the optimum content of the best catalyst is 7 g/L, which results in 98% removal of β -naphthol during 90 min.

4.4. Acidity effect

Fig. 8 illustrates the effect of photocatalytic degradation on β -naphthol by the best catalyst at various pH levels. The graph shows that the maximum removal occurs at pH 11 while the minimum removal takes place at acidic pH. This phenomenon can be attributed to the fact that although the maximum β -naphthol absorption on a catalyst occurs in neutral pH and then acidic pH because of the positive charges on the catalyst surface ($\text{pH}_{\text{pzc}} = 6.7$), in the main reactions of hydroxide radical generation (reactions 3 and 4), an increase in pH leads to generation of a larger number of hydroxide ions. Thus, at pH 11, wherein β -naphthol is in ionic form ($\text{p}K_{\text{a}} = 9.51$), the maximum β -naphthol removal is observed. Moreover, from pH 11 to 14,

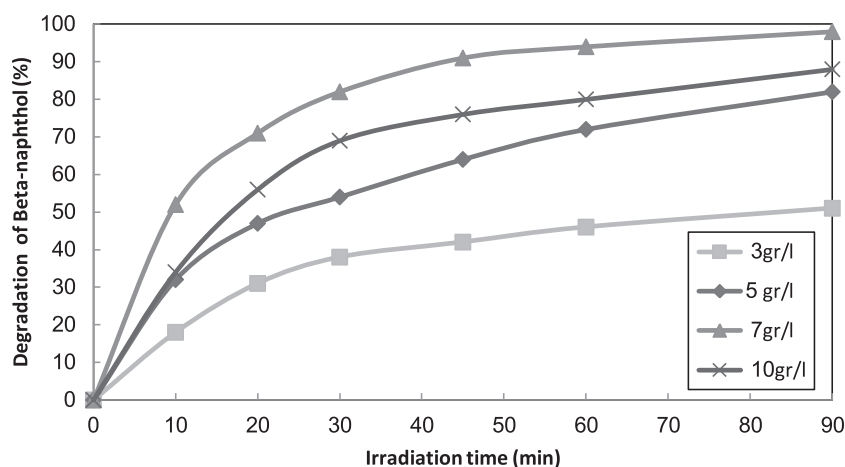


Fig. 7. Effect of the catalyst amount on the photocatalytic degradation of β -naphthol.

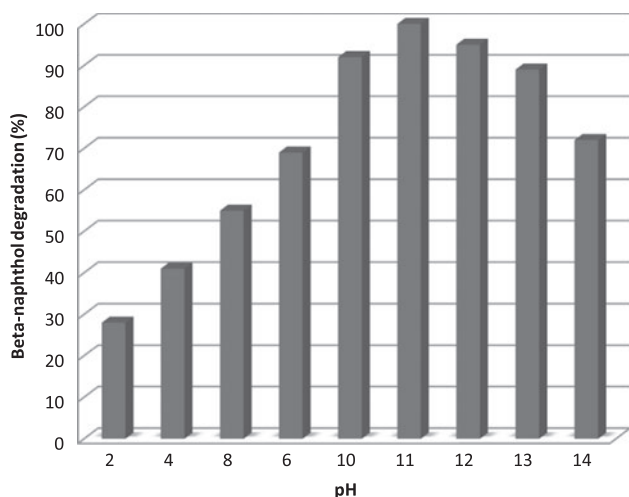
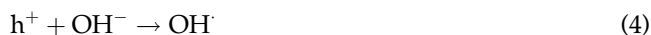
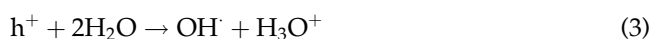


Fig. 8. Acidity effect on the photocatalytic degradation of β -naphthol.

β -naphthol removal decreases because of the competitive absorption among OH^- and β -naphthol ions.



4.5. Oxygen aeration effect

Fig. 9 presents oxygen aeration effect on β -naphthol degradation. As shown in the figure an increase in the aeration rate from 0.24 to 0.36 m^3/h leads to β -naphthol removal increase from 64.5 to 82%, and then this value drops. Hence, aeration rate of 0.36 m^3/h was selected as the optimum value in this work.

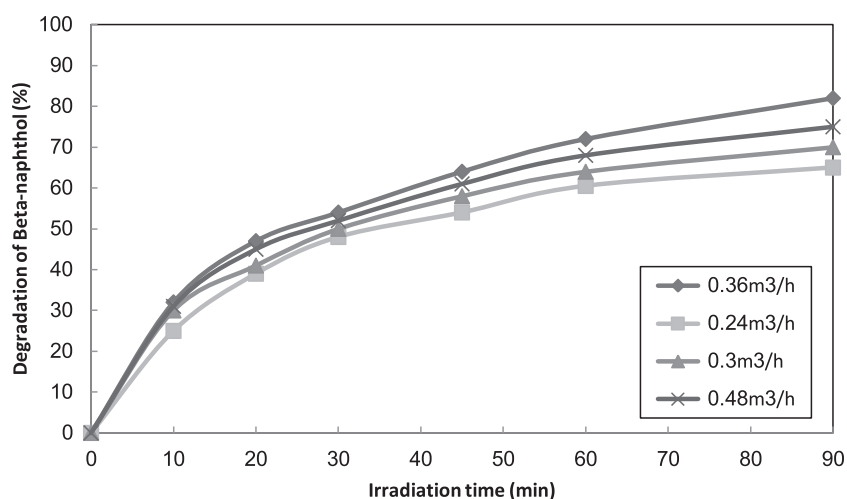


Fig. 9. Effect of aeration rate on the photocatalytic degradation of β -naphthol.

An increase in oxygen aeration rate from 0.24 to 0.36 m^3/h not only results in a better mixing in photo-reactor but also leads to the generation of more OH_2 and O_2^- ($\text{e}^- + \text{O}_2 \rightarrow \text{O}_2^- +$ and $\text{O}_2^- + \text{H}^+ \rightarrow \text{HO}_2$). Therefore, β -naphthol is degraded more easily. However, once this rate exceeds 0.48 m^3/h , the environment turbulence is severely increased and the generated bubbles prevent the complete transfer of UV in the reactor. As a result, the produced currents prevent the complete contact between catalyst and UV and it reduces the removal efficiency.

4.6. Effect of β -naphthol concentration

In this paper, various concentrations (1, 3, 5, and 7×10^{-3} mol/L) of β -naphthol were used to calculate the concentration effect. As shown in Fig. 10, once β -naphthol concentration rises from 1 to 7×10^{-3} mol/L, β -naphthol removal efficiency drops from 100 to 64%. This phenomenon can be attributed to the formation of multilayer β -naphthol around the catalyst at high concentrations. This multilayer is compacted and causes interruption in OH radical release through occupying the active spots on the catalyst surface. Besides, the high concentration of the contaminants reduces the photon penetration depth in the solution and, in turn, lowers the generation rate of OH radicals. Finally, the increased concentration of β -naphthol also decreases its removal efficiency.

4.7. Reaction kinetics

In this work, three processes are responsible for β -naphthol degradation: Photolysis, absorption, and



Fig. 10. Effect of the initial concentration of β -naphthol on its photocatalytic degradation.

photocatalyst. Fig. 11 illustrates these three processes separately and their synergic effect on β -naphthol degradation. As shown in the figure, TiO_2 -AC absorption process by itself leads to the minimum β -naphthol removal of 26%. AC absorption and photolysis process had contribution of 47 and 29%, respectively. Such a reduction can be attributed to the decreased surface area of AC since it is coated by nano- TiO_2 . The β -naphthol degradation rates were 52 and 82%, respectively, during the UV/AC and UV/ TiO_2 -AC processes. The results indicated that the maximum β -naphthol removal took place when integrating the absorption and the catalytic oxidation agents.

Due to the low concentration of the initial β -naphthol in this study, reaction kinetics are explained by pseudo-first-order Hinshelwood-Langmuir equation [36]:

$$R = k_r \theta = dC/dt = k_r \cdot k_a C / (1 + K_a C) \tag{5}$$

where: k_r is the actual rate of reaction which involves parameters such as catalyst amount, intensity of photons, amount of dissolved oxygen, acidity, etc.; k_a is the absorption constant. Once the initial concentration is low, $k_a C$ term is removed from denomination and Hinshelwood-Langmuir equation is transformed into a simpler form:

$$R = k_r \theta = dC/dt = k_r k_a t = K_{ap} t \tag{6}$$

where K_{ap} is the apparent rate of the contaminant.

The pseudo-first-order Hinshelwood-Langmuir equation is finally expressed as:

$$\ln(c/c_0) = -K_{ap} t \tag{7}$$

K_{ap} is calculated using the data from Fig. 11. Table 1 indicates the β -naphthol removal percentage, K_{ap} values, and the regression coefficient for various processes of this study. Here, the maximum rate is for

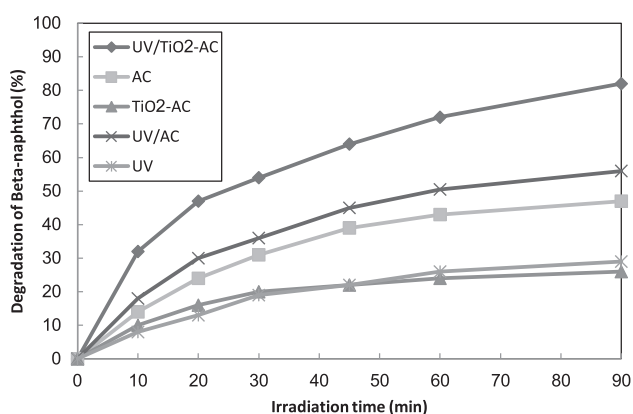
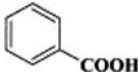
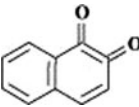
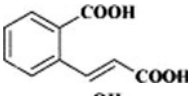
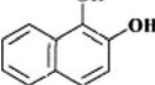
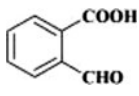
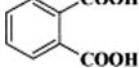


Fig. 11. A comparison among different photolysis, absorption, and photocatalytic processes during β -naphthol removal.

Table 1
Apparent first-order rate constant (K_{ap}) for different processes

Process	Removal percent	K_{app}	R^2
UV/ TiO_2 -AC	82	0.018	0.9725
UV/AC	56	0.0089	0.92
AC	47	0.007	0.8972
TiO_2 -AC	29	0.0037	0.9
UV	26	0.003	0.77

Table 2
Main reaction intermediate products identified by GC–MS

No	Structure	Name	Retention time (min)
i		Benzoic acid	16.6
ii		1,2-Naphthoquinone	19.2
iii		Trans-2-carboxybenzalpyravic acid	20.3
iv		1,2-Dihydroxynaphthalene	20.8
v		Formylbenzoic acid	21.1
vi		O-phthalic acid	22.7

UV/TiO₂-AC process with $K_{ap}=0.018$. Besides, photolysis process or TiO₂-AC had the minimum particle rate constant (regression).

The synergic effect of the process is shown by R which is calculated using the following equation:

$$R = K_{ap}UV/TiO_2 - AC / K_{ap}TiO_2 - AC \quad (8)$$

Substituting the apparent rate constant of absorption on TiO₂-AC and synergism photolysis of these two

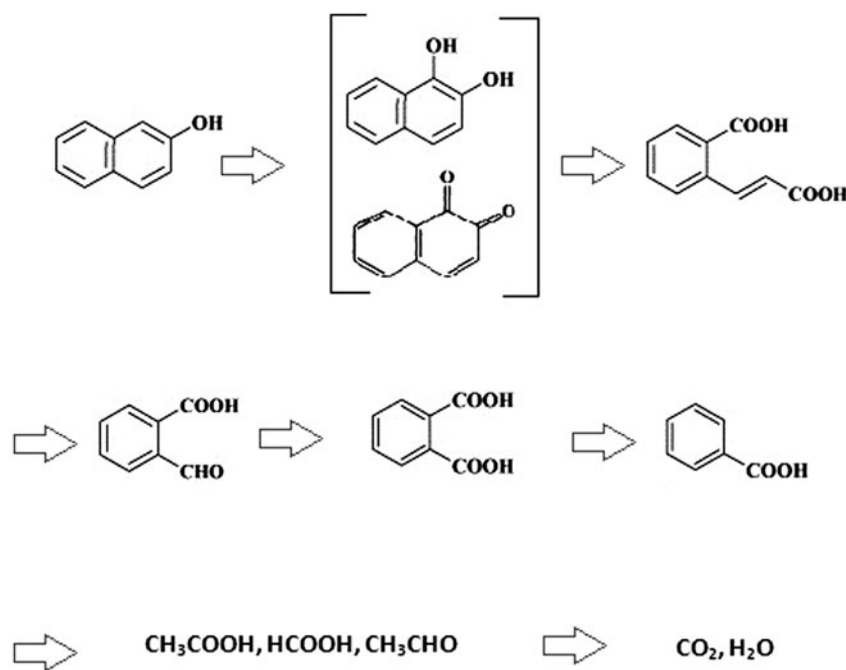


Fig. 12. Possible pathways for the formation of intermediates of the β -naphthol degradation.

processes, the value of 2.68 is obtained, which implies a strong synergism effect between the two photolysis and absorption processes.

4.8. Reaction trend

To identify β -naphthol degradation and the produced intermediate products during the reaction, GC-MS analysis was used. Table 2 indicates the obtained main peaks and the molecular structures. Considering the obtained products, the photocatalytic pathway of β -naphthol degradation is proposed as schematic illustration (Fig. 12).

As previously mentioned, by UV irradiation on surface of nano-TiO₂, electron and whole sites are created (reaction 5). These sites generate hydroxide and superoxide radicals through absorbing H₂O and oxygen (reactions 6 and 7). The radicals are highly active and lead to the oxidation of the contaminants. Synergism effect is rather weak on TiO₂-free surface of AC in the free radical and the OH radicals are generated with difficulty. However, after nano-TiO₂ stabilization on AC, UV irradiation results in the generation of a large number of OH radicals, which quickly oxidize the contaminant. The controlling mechanism of photocatalytic degradation in β -naphthol is based on the reactions (9–15):



By invasion of OH[·] radicals to β -naphthol, its structure was degraded and changed to 1,2-dihydroxy naphthalene and 1,2-dihydro naphthalene. Then, it was converted to 2-hydroxycinnamic acid and 2-ethanoxy benzoate compounds. By continuing the photocatalytic degradation process, the benzene cycle is broken and 1, 3-butanediol and, in the final stages, linear acetaldehyde, formic acid, and acetic acid are produced. Finally, β -naphthol is converted to H₂O and CO₂.

5. Conclusion

The results of this work indicated that TiO₂ nanoparticles with A/R = 4 have photocatalytic properties markedly more desirable than that of crystalline forms of anatase and other A/R ratios. In other words, AC containing nano-TiO₂ with A/R = 4 indicated higher removal efficiency, as compared to A/R = 2 and 1 and rutile crystals. Here, β -naphthol removal was performed in 90 min with removal efficiency of 100, 90, 68, 59, and 45, respectively. The reasonable increase in the catalyst content and the aeration rate resulted in enhanced β -naphthol removal; however, the further increase in these factors led to environment turbulence and a drop in the removal efficiency. Hence, the optimum catalyst content and aeration rate were determined as 8 g/L and 0.36 m³/h, respectively. The low concentration of the β -naphthol dramatically increased its removal efficiency, which is performed completely at concentration of 0.1 mM during less than 45 min. Both the hydrolysis synthesis of TiCl₄ for nanoparticle generation and thermal stabilization of TiO₂ on AC using the microwaves indicated high preparation speed and low prices and are appropriate approaches for synthesis of TiO₂ nanocatalysts with high photocatalytic properties. Using the nano-TiO₂ nanocatalysts stabilized on AC allows producing drinking water free from any chemical contaminants in a short time frame.

Acknowledgments

The authors are grateful to the Tarbiat Modares University for the support.

References

- [1] M.A. Lazar, S. Varghese, S.S. Nair, Photocatalytic water treatment by titanium dioxide: Recent updates, *Catalysts* 2 (2012) 572–601.
- [2] J.D. Meeker, L. Ryan, D.B. Barr, R. Hauser, Exposure to nonpersistent insecticides and male reproductive hormones, *Epidemiology* 17 (2006) 61–68.
- [3] A. Lair, C. Ferronato, J.M. Chovelon, J.M. Herrmann, Naphthalene degradation in water by heterogeneous photocatalysis: An investigation of the influence of inorganic anions, *J. Photochem. Photobiol. A: Chem.* 193 (2008) 193–203.
- [4] M. Antonopoulou, E. Evgenidou, D. Lambropoulou, I. Konstantinou, A review on advanced oxidation processes for the removal of taste and odor compounds from aqueous media, *Water. Res.* 53 (2014) 215–234.

- [5] B. Vaferi, M. Bahmani, P. Keshavarz, D. Mowla, Experimental and theoretical analysis of the UV/H₂O₂ advanced oxidation processes treating aromatic hydrocarbons and MTBE from contaminated synthetic wastewaters, *J. Environ. Chem. Eng.* 2 (2014) 1252–1260.
- [6] M. Yang, X. Liu, J. Chen, F. Meng, Y. Zhang, H. Brandl, T. Lippert, N. Chen, Photocatalytic and electrochemical degradation of methylene blue by titanium dioxide, *Chin. Sci. Bull.* 59 (2014) 1964–1967.
- [7] A. Fujishima, T.N. Rao, D.A. Tryk, Titanium dioxide photocatalysis, *J. Photochem. Photobiol. C: Photochem. Rev.* 1 (2000) 1–21.
- [8] U.I. Gaya, A.H. Abdullah, Heterogeneous photocatalytic degradation of organic contaminants over titanium dioxide. A review of fundamentals, progress and problems, *J. Photochem. Photobiol. C: Photochem.* 9 (2008) 1–12.
- [9] S.M. Gupta, M. Tripathi, A review of TiO₂ nanoparticles, *Chin. Sci. Bull.* 56 (2011) 1639–1657.
- [10] M. Pal, U. Pal, J.M.G.Y. Jiménez, F. Pérez-Rodríguez, Effects of crystallization and dopant concentration on the emission behavior of TiO₂: Eu nanophosphors, *Nanoscale. Res. Lett.* 7 (2012) 1–12.
- [11] B. Krishnakumar, K. Selvam, R. Velmurugan, M. Swaminathan, Influence of operational parameters on photodegradation of acid black 1 with ZnO, *Desalin. Water Treat.* 24 (2010) 132–139.
- [12] B. Subash, B. Krishnakumar, V. Pandiyan, M. Swaminathan, M. Shanthi, Synthesis and characterization of novel WO₃ loaded Ag-ZnO and its photocatalytic activity, *Mater. Res. Bull.* 48 (2013) 63–69.
- [13] N. Sobana, B. Krishnakumar, M. Swaminathan, Synergism and effect of operational parameters on solar photocatalytic degradation of an azo dye (Direct Yellow 4) using activated carbon-loaded zinc oxide, *Mater. Sci. Semicond. Process.* 16 (2013) 1046–1051.
- [14] B. Krishnakumar, T. Imae, J. Miras, J. Esquena, Synthesis azo dye photodegradation activity of ZrS₂-ZnO nano-composites, *Sep. Purif. Technol.* 132 (2014) 281–288.
- [15] C. Duarte, M. Sampa, P. Rela, H. Oikawa, C. Silveira, A. Azevedo, Advanced oxidation process by electron-beam-irradiation-induced decomposition of pollutants in industrial effluents, *Radiat. Phys. Chem.* 63 (2002) 647–651.
- [16] A. Khataee, V. Vatanpour, A. Amani Ghadim, Decolorization of C.I. Acid Blue 9 solution by UV/Nano-TiO₂, Fenton, Fenton-like, electro-Fenton and electrocoagulation processes: A comparative, *J. Hazard. Mater.* 161 (2009) 1225–1233.
- [17] L. Sun, J.R. Bolton, Determination of the quantum yield for the photochemical generation of hydroxyl radicals in TiO₂ suspensions, *J. Phys. Chem.* 100 (1996) 4127–4134.
- [18] C. Wong, W. Chu, The direct photolysis and photocatalytic degradation of alachlor at different TiO₂ and UV sources, *Chemosphere* 50 (2003) 981–987.
- [19] W. Wu, X. Xiao, S. Zhang, F. Ren, C. Jiang, Facile method to synthesize magnetic iron oxides/TiO₂ hybrid nanoparticles and their photodegradation application of methylene blue, *Nanoscale. Res. Lett.* 6 (2011) 1–15.
- [20] S. Qourzal, A. Assabbane, Y.A. Ait-Ichou, Synthesis of TiO₂ via hydrolysis of titanium tetraisopropoxide and its photocatalytic activity on a suspended mixture with activated carbon in the degradation of 2-naphthol, *J. Photochem. Photobiol. A Photochem.* 163 (2004) 317–321.
- [21] S. Qourzal, N. Barka, M. Tamimi, A. Assabbane, Y. Ait-Ichou, Photodegradation of 2-naphthol in water by artificial light illumination using TiO₂ photocatalyst: Identification of intermediates and the reaction pathway, *Appl. Catal. A: Gen.* 334 (2008) 386–393.
- [22] S. Qourzal, N. Barka, M. Tamimi, A. Assabbane, A. Nounah, A. Ihlal, Y. Ait-Ichou, Sol-gel synthesis of TiO₂ SiO₂ photocatalyst for β-naphthol photodegradation, *J. Mater. Sci. Eng.: C* 29 (2009) 1616–1620.
- [23] S. Qourzal, M. Tamimi, A. Assabbane, Y. Ait-Ichou, Photocatalytic degradation and adsorption of 2-naphthol on suspended TiO₂ surface in a dynamic reactor, *J. Colloid. Interface Sci.* 286 (2005) 621–626.
- [24] S. Qourzal, M. Tamimi, A. Assabbane, Y. Ait-Ichou, Photodegradation of 2-naphthol using nanocrystalline TiO₂, *M. J. Condensed. Mater.* 11 (2009) 55–59.
- [25] S. Weng, Z. Pei, Z. Zheng, J. Hu, P. Liu, Exciton-free, nonsensitized degradation of 2-naphthol by facet-dependent biocd under visible light: Novel evidence of surface-state photocatalysis, *ACS. Appl. Mater. Interfaces* 5 (2013) 12380–12386.
- [26] N. Daneshvar, D. Salari, A. Khataee, Photocatalytic degradation of azo dye acid red 14 in water: Investigation of the effect of operational parameters, *J. Photochem. Photobiol. A: Chem.* 157 (2003) 111–116.
- [27] J.M. de Souza e Silva, M. Pastorello, M. Strauss, C.M. Maroneze, F.A. Sigoli, Y. Gushikem, I.O. Mazali, Size controlled synthesis of highly dispersed anatase/rutile nanoparticles with photocatalytic activity toward salicylic acid degradation, *RSC. Adv.* 2 (2012) 5390–5397.
- [28] Y.H. Jung, K.H. Park, J.S. Oh, D.H. Kim, C.K. Hong, Effect of TiO₂ rutile nanorods on the photoelectrodes of dye-sensitized solar cells, *Nanoscale. Res. Lett.* 8 (2013) 1–6.
- [29] X. Zhou, J. Lu, J. Jiang, X. Li, M. Lu, G. Yuan, Z. Wang, M. Zheng, H.J. Seo, Simple fabrication of N-doped mesoporous TiO₂ nanorods with the enhanced visible light photocatalytic activity, *Nanoscale. Res. Lett.* 9 (2014) 1–7.
- [30] T. Zhang, L. Liu, F. Yang, Y. Wang, J. Kang, Improved conversion efficiency of dye-sensitized solar cells by using novel complex nanostructured TiO₂ electrodes, *Sci. Chin. Technol. Sci.* 56 (2013) 115–119.
- [31] B. Tan, Y. Zhang, M. Long, Large-scale preparation of nanoporous TiO₂ film on titanium substrate with improved photoelectrochemical performance, *Nanoscale. Res. Lett.* 9 (2014) 1–6.
- [32] T.L. Thompson Jr., J.T. Yates Jr., Surface science studies of the photoactivation of TiO₂-new photochemical processes, *Chem. Rev.* 106 (2007) 4428–4453.
- [33] S. Kittaka, K. Matsuno, S. Takahara, Transformation of ultrafine titanium dioxide particles from rutile to anatase at negatively charged colloid surfaces, *J. Solid. State. Chem.* 132 (1997) 447–450.
- [34] J.H. Lee, Y.S. Yang, Effect of HCl concentration and reaction time on the change in the crystalline state of

- TiO₂ prepared from aqueous TiCl₄ solution by precipitation, *J. Eur. Ceram. Soc.* 25 (2005) 3573–3578.
- [35] Q.H. Zhang, L. Gao, J.K. Guo, Preparation and characterization of nanosized TiO₂ powders from aqueous TiCl₄ solution, *Nanoscale. Res. Lett.* 11 (1999) 1293–1300.
- [36] M. Behnajady, N. Modirshahla, R. Hamzavi, Kinetic study on photocatalytic degradation of C.I. acid yellow 23 by ZnO photocatalyst, *J. Hazard. Mater.* 133 (2006) 226–232.